



Prof. Hoda Abd El Kader Saleh

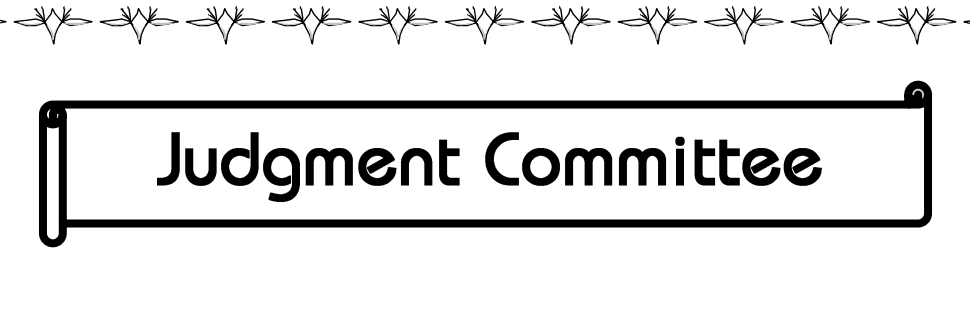
Professor of Oral and Maxillofacial Radiology
Faculty of Dentistry
Cairo University

Dr. Iman Ismail Dakhli

Associate Professor of Oral and Maxillofacial Radiology

Faculty of Dentistry

Cairo University



Dr. Mary Medhat Farid

Associate Professor of Oral and Maxillofacial Radiology Faculty of Dentistry

Ain Shams University

Prof. Hany Omar

Professor of Oral and Maxillofacial Radiology
Faculty of Dentistry
Cairo University

Prof. Hoda Abd El Kader Saleh

Professor of Oral and Maxillofacial Radiology,

Faculty of Dentistry

Cairo University

Before all and above all, thanks to Allah for everything

I would like to express my deepest gratitude and appreciation to **Prof. Hoda Abd El Kadr Saleh**, professor of Oral & Maxillofacial Radiology, Faculty of Oral and Dental Medicine, Cairo University, for her valuable guidance, instructive supervision, and sincere encouragement.

I'm also thankful for **Dr. Iman Ismail Dakhli**, associate professor Oral & Maxillofacial radiology, Faculty of oral and Dental Medicine, Cairo University, for her guidance and for directing me throughout the study.

Finally, I would like to thank all the **staff members** of the Oral Radiology Department, Faculty of Oral and Dental Medicine, Cairo and MTI University for their excellent support and cooperation





To my **father**, who taught me that the best kind of knowledge to have is that which is learned for its own sake and who taught me that even the largest task can be accomplished if it is done one step at a time.

To my **mother**, who taught me to make reading and learning a basic part of my personality, for her encouragement and inspiration to me throughout my life, and for providing a 'writing space'. To my **big family** whom made me very grateful to be a member of them.





list of Contents

label	Page number
List of Abbreviations	I
List of Tables	III
List of Figures	VI
Introduction	
Review of Literature	3
Endodontic Strategies for Root Cana	lls Identification10
Radiographic Methods for Root Can	al System Assessment17
Principles of Cone-Beam Computed	Tomographic Imaging23
Strengths and Limitations	39
CBCT Artifacts	41
Application of CBCT Imaging to Clin	nical Dental Practice47
PIRT and Research Question	67
Aim of The Study	69
Subject & Methods	70
I. Tooth Sectioning:	70
II. Image Evaluation:	73
Statistical Analysis	81
Results	82
Discussion	102
Summary and Conclusion	109
Recommendations	111
References:	112
الملخص العربي	131

list of Abbreviations

MB1	First Mesiobuccal Root Canal
MB2	Second Mesiobuccal Root Canal
MB3	Third Mesiobuccal Root Canal
3D	Three-Dimensional
2D	Two-Dimensional
CBCT	Cone-Beam Computed Tomography
CT	Computed Tomography
μCΤ	Micro Computed Tomography
MRI	Magnetic Resonance Image
CCD/ IIT	Charge-Coupled Device/ Image Intensifier Tube
FPD	Flat Panel Detector
CsI	Cesium Iodide
MPR	Multiplanar Reformation
DVR	Direct Volume Rendering
IVR	Indirect Volume Rendering
MIP	Maximum Intensity Profile
DICOM	Digital Imaging and Communications in
	Medicine
MSCT	Multi-Slice Computed Tomography
MDCT	Multi-Detector Computed Tomography
TMJ	Temporomandibular Joint
SNR	Signal to Noise Ratio
CNR	Contrast to Noise Ratio
VRF	Vertical Root Fractures
HRF	Horizontal Root Fractures
RCs	Root Canals
IADT	International Association of Dental
	Traumatology
AAE	American Association of Endodontists
AAOMR	American Academy of Oral and Maxillofacial
	Radiology
ERR	External Root Resorption

IAN	Inferior Alveolar Nerve
ULD	Ultra Low Dose
LED	Light-Emitting Diode
EDTA	Ethylenediaminetetra Acetic Acid
SOM	Surgical Operating Microscope
ROI	Region of Interest
ALARA	As Low As Reasonably Achievable
SD	Standard Deviation
AUC	Area Under Curve
ROC	Receiver Operating Characteristic Curve
FN	False Negative
FP	False Positive
PPV	Positive Predictive Value
NPV	Negative Predictive Value
PIRT	P: Population
	I: Index
	R: Reference
	T: Target

list of Tables

Table 1: Detection of MB2 canal using 0.3 voxel size CBCT reformatted images versus root sectioning by observer 1	83
Table 2: Detection of MB2 canal using 0.3 voxel size CBCT reformatted images versus root sectioning by observer 2	84
Table 3: Detection of MB2 canal using 0.3 voxel size CBCT reformatted images versus root sectioning by observer 3	85
Table 4: Diagnostic accuracy of 0.3mm CBCT voxel size rating detection of MB2 canal versus root sectioning by all of the three observers	e
Table 5: Detection of MB2 canal using 0.2 voxel size CBCT reformatted images versus root sectioning by observer 1	86
Table 6: Detection of MB2 canal using 0.2 voxel size CBCT reformatted images versus root sectioning by observer 2	87
Table 7: Detection of MB2 canal using 0.2 voxel size CBCT reformatted images versus root sectioning by observer 3	88
Table 8: Diagnostic accuracy of 0.2mm CBCT voxel size rating detection of MB2 canal versus root sectioning by all of the three observers	
Table 9: Detection of MB2 canal using 0.125 voxel size CBCT reformatted images versus root sectioning by observer 1	90

Table 10: Detection of MB2 canal using 0.125 voxel size CBCT
reformatted images versus root sectioning by observer 29
Table 11: Detection of MB2 canal using 0.125 voxel size CBCT
reformatted images versus root sectioning by observer 39
T 11 12 D
Table 12: Diagnostic accuracy of 0.125mm CBCT voxel size rating in
detection of MB2 canal versus root sectioning by all of the three
observers9
Table 12. Overall diagnostic accuracy of all CDCT years sizes noting
Table 13: Overall diagnostic accuracy of all CBCT voxel sizes rating in detection of MB2 canal versus root sectioning by all of the three
observers9
OUSELVELS
Table 14: Fleiss Kappa results of inter-observer agreement for 0.3,
0.2 and 0.125 CBCT voxel sizes9
Table 15: Detection of MB2 canal using 0.3 voxel size CBCT
reformatted images versus root sectioning (Inter-observer
agreement)9
Table 16: Shown Sensitivity, Specificity, PPV, NPV, MB2 prevalence
Diagnostic Accuracy, AUC and 95% CI of 0.3 CBCT voxel size9
Diagnostic recurrecy, rice and so to or one obot voice size
Table 17: Detection of MB2 canal using 0.2 voxel size CBCT
reformatted images versus root sectioning (Inter-observer
agreement)9
ugi coment)
Table 18: Shown Sensitivity, Specificity, PPV, NPV, MB2 prevalence
Diagnostic Accuracy AUC and 95% CI of 0.2 CBCT voxel size9

Table 19: Detection of MB2 canal using 0.125 voxel size CBCT reformatted images versus root sectioning (Inter-observer agreement)	.98
Table 20: Shown Sensitivity, Specificity, PPV, NPV, MB2 prevalence	
Diagnostic Accuracy AUC and 95% CI of 0.125 CBCT voxel size	99
Table 21: Comparison among the different CBCT voxel sizes (0.3, 0 and 0.125) versus root sectioning AUC in detection of MB2 canal1	

list of Figures

Figure 1: Diagram showing maxillary molar with 4 canals: first
mesiobuccal canal (MB1), secondary mesiobuccal canal (MB2),
distobuccal canal (DB) and palatal canal (P). A; Maxillary molar
with joining mesiobuccal canals. B; Maxillary molar with two
separate mesiobuccal canals4
Figure 2: Diagram showing classification of multiple canals in MB
root of the maxillary molar tooth by Weine et al. Type I, Type II,
Type III and Type IV were later expanded to include Type V
configuration6
Figure 3: Diagram showing root canal classifications by Vertucci7
rigure 3. Diagram showing root canar classifications by vertacer
Figure 4: Diagram showing root canal classifications by Gulabivala
et al 20019
Figure 5: Showing two mesial canals are distinguishable in the
mandibular right first molar using two radiographs taken with the
parallax technique, also note how the periapical radiolucent lesions
change in size and radio-opacity with a change of angulation of the
X-ray tube head18
Figure 6: Showing a case where the palatal vault is not high enough
to allow the film to lie parallel to the long axis of the tooth resulting
in distortion of the image even though a beam-aiming device has been
used

Figure 7: Showing (a) The zygomatic arch is obscuring the apical anatomy of the maxillary molar teeth, (b) the radiolucent lesion (yellow arrow) on the mesial aspect of the mesiobuccal root may be difficult to accurately assess as it is superimposed over the radiolucent maxillary sinus
Figure 8: Showing (a) This mandibular left molar tooth immediately after completion of root canal treatment, (b) the tooth is reviewed 6 months later, there appears to be no change is the size of the periapical radiolucency, (c) if the angle of the X-ray tube head is changed by 10° there are definite signs of periapical healing20
Figure 9: Showing x-ray beam projection scheme comparing acquisition geometry of cone beam imaging (left) with conventional 'fan beam' CT (right)23
Figure 10: Showing, cone-beam imaging geometry25
Figure 11: Showing, classification of CBCT units according to the FOV. A, Large FOV scans provide images of the entire craniofacial skeleton, enabling cephalometric analysis. B, Medium FOV scans image the maxilla or mandible or both. C, Focused or restricted FOV scans provide high-resolution images of limited regions. D, Stitched scans from multiple focused FOV scans provide larger regions of interest to be imaged from superimposition of multiple scans30
Figure 12: Showing, display mode options of CBCT volumetric data39
Figure 13: Showing, axial view demonstrating beam hardening (dark bands), scatter (white streaks), and cupping (image distortion) artifacts
Figure 14: Showing, pictorial plot of the effect of number of basis projection images. (A) Increasing number of projections provides

more data and reduces image noise. (B) Reducing the number of projections creates undersampling and produces streaks43
Figure 15: Showing, blurring and double cortices (arrows) caused by motion artifact44
Figure 16: Showing, schematic of cone-beam related artifact. Centrally, the amount of data acquired is maximal, whereas peripherally (transparent blue), the amount of data collected is
appreciably less, producing artifacts of increased noise, distortion, and reduced contrast45
Figure 17: Showing, circular or ring artifact46
Figure 18: Showing, CBCT imaging for implant site assessment. Reformatted panorama with thin slice image (B), serial thin-slice cross-section images (C)
Figure 19: Showing, CBCT in diagnosis of localization of impacted teeth and identification of associated upper left canine root resorption which shown in C49
Figure 20: Fusion image. Three-dimensional anatomic views demonstrate imaging possibilities with fusion of CBCT data and photographic image sets
Figure 21: (A) Axial and (B) sagittal CBCT images showing large lingual tonsils (black arrow) narrowing the airway of a patient51
Figure 22: CBCT showing, a dome-shaped lesion arising from the floor of the Rt sinus, without mucosal thickening of the rest of the sinus, findings which is characteristic of a retention pseudocyst52